

Grain characteristics and engineering properties of coal ash

A. Trivedi, V. K. Sud

Abstract Ash produced by the coal fired thermal plants is often used as a geo-material where its characteristics and mechanical behavior is important. The present study describes an investigation into the grain characteristics and the engineering properties of coal ash. The results of x-ray diffraction, micrographic observation and grain size distribution are analyzed in relation to maximum and minimum void ratio, permeability, compressibility and frictional properties. The grain size is found to be a significant grain characteristic that may be used for classification of ash as well as interpretation of primary, secondary and index properties. The compressibility and frictional characteristics depend on stress environment and packing with respect to a critical state uniquely identified by material characteristics. The fitting parameters for the selected sets of samples have been evaluated for the Ropar coal ash. This study presents the data and the correlations that are pertinent to a wider community of geo-technical and geo-environmental engineers interested in the utilization of coal ash as a structural fill.

Keywords Grain size, Primary, Secondary and index properties, Compressibility, Critical state, Structural fill

Received: 13 March 2002

A. Trivedi (✉)
Assistant Professor, Civil Eng.,
Thapar Institute of Engineering & Technology
(Deemed University), Patiala, India, 147004
e-mail: atrivedi14@yahoo.com

V. K. Sud
Formerly Visiting Professor,
Thapar Institute of Engineering & Technology
(Deemed University), Patiala, India, 147004

This material is based upon a study supported by the doctoral thesis and project work on coal ash at Thapar Institute of Engineering and Technology, Patiala, India. Any opinion, findings and conclusions expressed in this material are valid within the sample set and do not necessarily reflect the behavior of all the ashes. The suggestions of *Prof. Sundar Singh*, department of civil engineering, TIET, Patiala, and his useful insight in critical state behavior of coal ash are greatly appreciated. The assistance of numerous postgraduate students in sampling is thankfully acknowledged.

Introduction

Coal ash is identified as a material produced by the burning of coal in large quantities by coal fired thermal power plants. The ash is stored in large ash ponds constructed in the vicinity of the thermal plants. It is used as a structural fill in the ash dikes. Until recently, the modeling of the mechanical behavior of ash has remained case specific, but it is now recognized that its constitutive behavior is largely determined by its particle size distribution and grain characteristics. The physical, chemical and mechanical properties of the coal ash depend on the coal type, its origin, handling, grain size, processing technique, boiler size, disposal and storage methods, etc. Due to a large variety of the coal ash types and morphology, the engineering behavior of coal ash is complex to model. The engineering behavior of coal ash such as non-linear deformation, dilatancy, and permeability is influenced by the physical properties and the environmental conditions. The grain size characteristics may be used for classification of ash as well as for the interpretation of primary, secondary and index properties. The primary and secondary physical properties of soils have been categorized by Spronck [1]. Miura et al. [2] studied primary physical characteristics and their influence on the index properties of sands. Iwasaki and Tatsuoka [3] investigated the effect of grain sizes on the shear modulus of sands.

The primary properties focus upon permanent features of the ash type such as its morphology, specific gravity, shape and distribution. Secondary properties are changeable parameters such as packing, orientation of grains, bulk density, void ratio, and permeability, etc. The index properties include the maximum and the minimum void ratio, and the angle of repose, etc. The critical angle is often described as mineralogical-morphological parameter [4]. The peak friction angle is recognized as an environmental effect of the stress state and the packing with respect to a critical state uniquely identified by the material characteristics [4]. In this study, as a matter of interest to geotechnical and geo-environmental engineers, the effect of grain characteristics on the properties and the mechanical behavior of representative ash samples from various storage locations of the Ropar thermal power plant Punjab, India have been discussed. Utmost care was taken so that test sample sets were representative of the grain size distribution and characteristics as described. These samples were collected in polyethylene bags and sealed at the location of collection.

Sample characteristics

The samples A1 and A2 were collected from an ash pond where they were disposed by a wet method in the form of slurry. The samples referred as B1 to B7 were collected in dry state from different hoppers of the electrostatic precipitators. The sample A3 was obtained as the dry mixture of the ashes from different hoppers.

The grain sizes present in various ash samples were obtained from the mechanical sieve shaker and the hydrometer analysis. All the ash samples were passed through mechanical sieves of aperture 4.75, 2.36, 1.2, 0.6, 0.3, 0.15, and 0.075 mm, arranged in this order. The ash fraction passing through 0.075 mm was collected on a pan and was used in a hydrometer test for the analysis of fines. Different samples were grouped as coarse grained (A1, A2, B1, B2, B3) and fine grained ashes (A3, B4, B5, B6, B7). Studies were carried out for a minimum of three samples, collected from each location referred to above, producing consistent results. The grain size analysis plot was transferred as five equivalent sizes corresponding to 0, 10, 50, 80, and 100% finer by weight for each of the ashes shown (Fig. 1a & b). The samples were designated coarse and fine having mean sizes in the range of 200 to 70 and 25 to 5 μm respectively. The coarse (Fig. 1a) and the fine (Fig. 1b) samples were having sizes between 4000 and 9 and 1000 and 1 μm respectively. Particle size distribution studies show that the mean size of particles may generally vary from less than 200 to 5 μm in diameter.

Ash ranges in size from silt, sandy silt to sand as observed by Leonards and Bailey [5], Toth et al. [6], Skarzynska et al. [7], Dayal [8], Sridharan et al. [9], Trivedi [10] and Trivedi et al. [11]. Pond ashes (A1, A2) have higher specific gravity (either due to weathering reactions or the presence of bottom ash) compared to the ashes collected dry from the ESP (electrostatic precipitator) even though

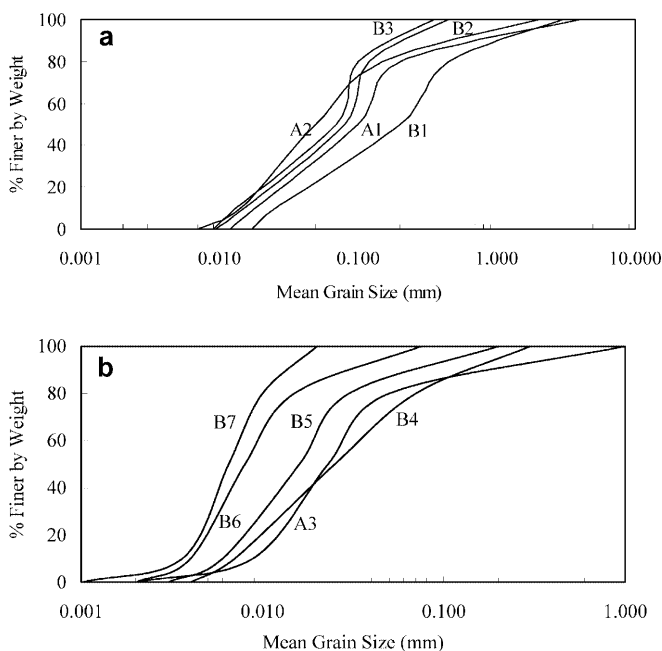


Fig. 1. (a) Grain size distribution of coarse coal ashes. (b) Grain size distribution of fine coal ashes

having similar mean size (B1, B2). The coefficient of uniformity for the coarse samples varied between 10 to 5 and that of the fine samples between 6 to 2 (Fig. 2). The coefficient of uniformity is defined as a ratio of D_{60} and D_{10} . D_{60} and D_{10} are sizes corresponding to that 60 and 10% ash being finer by weight. Although firing conditions will have some effect on the grading of the ash produced, it is likely that for any power station, initial pulverization of coal and sedimentation in lagoons, has the greatest influence on the grading of the ash. Thus coarse-grained ashes have a higher coefficient of uniformity than the fine samples (Fig. 2). In the ash ponds the ash is deposited along a gradient, which also occur due to particle size separation along the beach. The coarse material containing bottom ash settles first. It drains rapidly in the pond. It has higher grading compared to the particle size distribution of samples collected from the ESP (Series-B).

Structure, particle shape and composition

Coal ash is derived from a natural material, and as such, its composition depends upon the type of coal used in the thermal power stations. The rock detritus in the coal is likely to vary from one coal sample to the other [12], so that variations are expected among the ashes. In the burning chamber subdivision and decomposition occur [13]. The mineral groups present in the coal are hydrated silicate (clay minerals e.g. kaolinite, montmorillonite, and muscovite), carbonate (calcite, siderite, and dolomite), sulphate (gypsum anhydrate), silicate (e.g. quartz and feldspar), phosphate (apatite), sulphide (pyrite and marcasite). The minerals in coal and their varying proportion generally play a major role in determining the chemical composition of the ash [14]. During combustion as the coal passes through the high temperature zone in the furnace, the volatile matter and carbon are burned out whereas most of the mineral impurities will melt at high temperature. The base metal sulphides are mainly responsible for flue gases and S-content of the ash. The fused matter produced in the furnace is quickly transported to lower temperature zones, where it solidifies as almost spherical particle of the silicate glass. Some of the mineral matter agglomerate forms bottom ash, but the most of it flies out with the flue gas stream and is called fly ash. Coal ash is subsequently removed from the gas by ESP.

The present ash containing less than 10% lime is generally a product of combustion of anthracite, bituminous, and sub-bituminous coal. In the furnace, when large spheres of molten glass do not get cooled rapidly and uni-

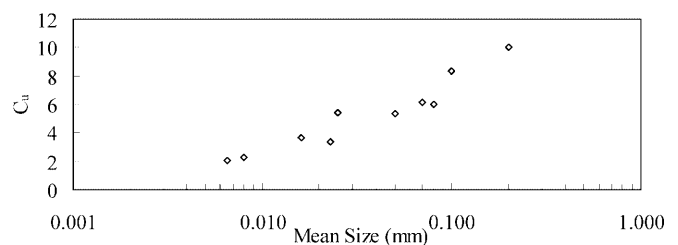


Fig. 2. Variation of coefficient of uniformity (C_u) with mean size

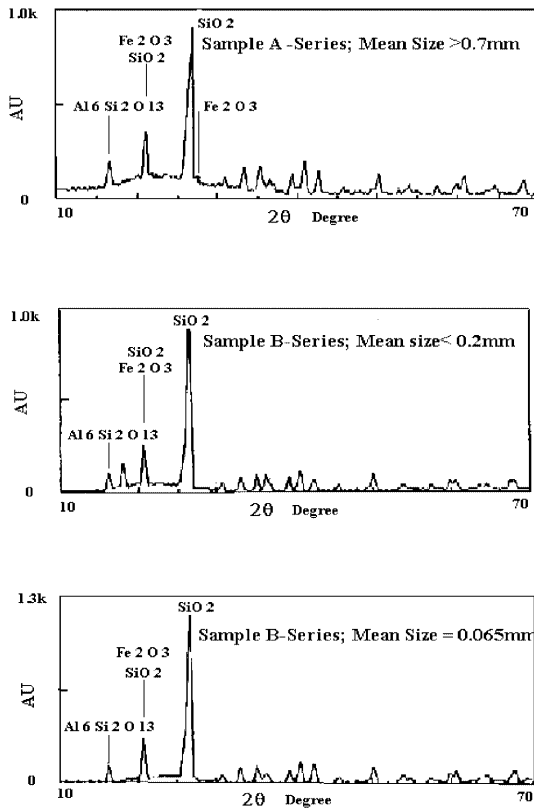


Fig. 3. X-ray diffraction pattern of coal ash

formly, sillimanite ($\text{Al}_2\text{O}_3 \cdot \text{SiO}_2$) or mullite ($3\text{Al}_2\text{O}_3 \cdot \text{SiO}_2$) may crystallize as slender needles in the interior of the glassy spheres. X-ray diffraction analyses have confirmed that the principal crystalline minerals in coal ashes are quartz, mullite, hematite, and magnetite (Fig. 3). These crystalline minerals are non-reactive at ordinary temperatures; their presence in large proportion tends to reduce its reactivity. These ashes practically behave as an inert material.

The chemical composition of the ash is determined by the chemical composition of the non combustible components in the coal. Different minerals in coal with a constant overall chemistry will result in ashes of the same chemical composition but may lead to different mineralogical composition. The chemical analysis of Ropar ash indicates SiO_2 (57.5%), Al_2O_3 (27.2%), Fe_2O_3 (5.4%), CaO (3.1%), MgO (0.4%), soluble ($\sim 1\%$), and unburned carbon ($\sim 4\%$ by weights). It has been reported that the mechanical properties of ash depend on the grain size, shape and distribution. Micrographic observation (Fig. 4) indicates the existence of the following constituents in ash (i) clear and brownish glass spheres, (ii) sub rounded porous grains, (iii) irregular agglomerates, (iv) opaque spheres or angular grains of magnetite (dark gray) and hematite (red) identified by their color, (v) irregular porous grains of unburned carbon (black). Micrographic evidence suggests that most of the particles in fly ash occur as solid spheres of glass. In addition a small number of hollow spheres, which are called cenospheres (completely empty) and plerospheres (packed with numerous small spheres or crystals) may be present.

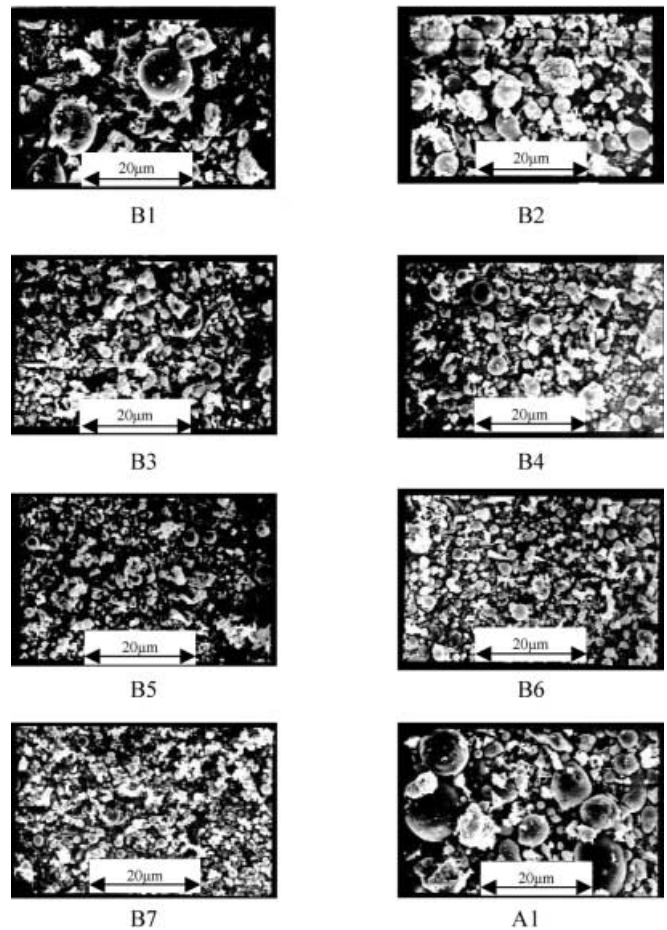


Fig. 4. Electron micrograph of typical ash samples

Apparent specific gravity

In the present study the apparent specific gravity was obtained with a pycnometer. Compared with natural soils having specific gravity in the range of 2.5 to 2.7, coal ashes have low apparent specific gravity (G_a , 1.6 to 2.1) (Fig. 5). The specific gravity of the ash is a function of both chemical constituents and fineness. The specific gravity of various individual chemical components namely nepheline or $\text{Na}_2\text{O} \cdot \text{Al}_2\text{O}_3 \cdot \text{SiO}_2$ (G_s , 2.5 to 2.6), mullite or $3\text{Al}_2\text{O}_3 \cdot 2\text{SiO}_2$ (G_s , 3.1 to 3.6), quartz or SiO_2 (G_s , 2.65), hercynite or $\text{FeO} \cdot \text{Al}_2\text{O}_3$ (G_s , 3.5 to 4.1), fayalite or $2\text{FeO} \cdot \text{SiO}_2$ (G_s , 4.3), hematite or Fe_2O_3 (G_s , 4.9 to 5.3) and magnetite or Fe_2O_3 (G_s , 5.18) is higher than the apparent specific gravity of coal ash because of different arrangements in their solid state. It is apparent that ash with high iron content (Fe_2O_3) will have a corresponding-

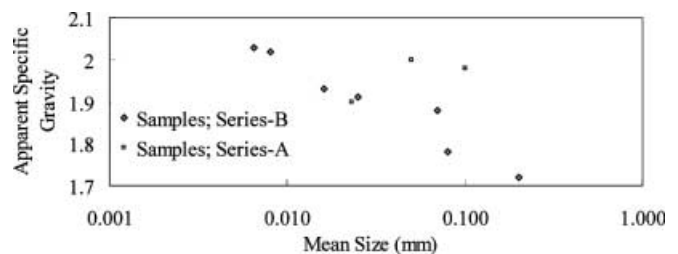


Fig. 5. Apparent specific gravity plotted against mean size

ly high specific gravity [15]. Lower values for floating scum (0.8) are attributed to high concentration of cenospheres. The cenospheres and plerospheres are also observed in the non-floating coarser fraction of the coal ash. The specific gravity of pond ash in the discharge zone (2.17) is reported to be higher than that of out flow and transition zone (2.13 to 2.06) [7], because of the concentration of bottom ash in the discharge zone. Pandian et al. [16] reported a variation of specific gravity in relation to the grain size (G_a , 1.6 to 1.9, for Korba pond ash) and iron content (G_a , 1.6 to 2.0 for iron content between 3.5 to 9%). The specific gravity of in situ (2.27) and powdered ash (2.36) samples [5] suggested an increase in the apparent values due to breaking of the coarse ash to the fine one. The apparent specific gravity decreases with the mean particle size of the ash material (Fig. 5). There is a sporadic scatter of apparent specific gravity values of pond ash due to the presence of bottom ash.

Maximum and minimum void ratio

The maximum and the minimum void ratios depend on the grain properties and the state of compaction. The maximum void ratio was determined by a slow pouring technique. The minimum void ratio was obtained by pouring ash in a standard mold with a volume of 2,830 cm³ using a thick walled cylindrical tube. The maximum density was achieved by densifying dry ash in this mold using an electromagnetic, vertically vibrating table with a frequency of 60 Hz. For fine ashes (Fig. 1b) difficulties of the flow of fines were encountered in using this technique. The capping plate was modified to fit at the top of the mold. Double amplitude of vertical vibration of 0.38 mm was found to be optimal for all the ash samples. The careful execution of this procedure leads to a reasonably reproducible value. Figure 6 gives both the maximum and the minimum densities of various ash samples. Fine ashes tend to have a higher maximum density than the coarse ash of parallel gradation (B2 & B3). An increasing coefficient of uniformity for the common mean particle size (A3 & B4) increases the maximum density.

All ash samples were compacted in a Proctor standard mold and the void ratio was determined. The

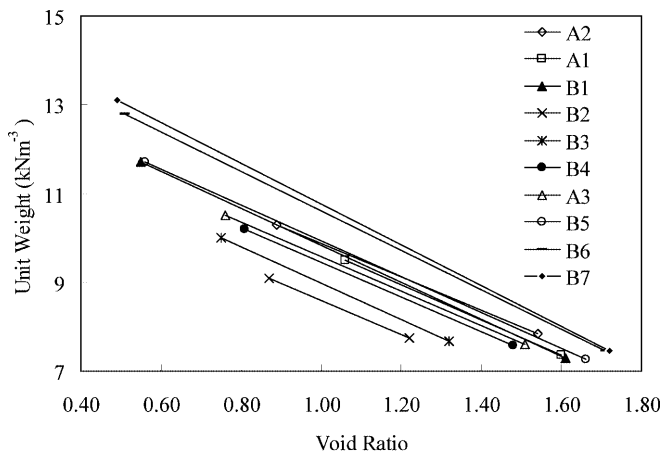


Fig. 6. Variation of unit weight of coal ashes with void ratio

minimum void ratio corresponding to the maximum density achieved in a dry vibration and the Proctor compaction test is compared (Fig. 7) for various ash samples. A lower void ratio is obtained essentially in the dry vibration test. The difference between the void ratio in dry vibration and Proctor compaction decreases with increasing mean size and becomes insignificant for the coarse ash samples (Fig. 7). This difference is attributed to slacking of ash due to the presence of moisture in the Proctor test. Breaking of cenospheres is observed in the modified Proctor test due to greater impact. The difference between the maximum and the minimum void ratio, defined as void ratio extent, is plotted for various ashes (Fig. 8). There is a gradual reduction of the void ratio extent with the increasing mean size. The ratio of maximum and minimum void ratios has been plotted to find a relation with the mean size. The trend line (shown in Fig. 9) indicates a satisfactory coefficient of reliability of 0.9 in the relation

$$e_{\max} = n.e_{\min} (\text{mean size})^{-m}, \tag{1}$$

where $m = 0.3$ and $n = 0.82$.

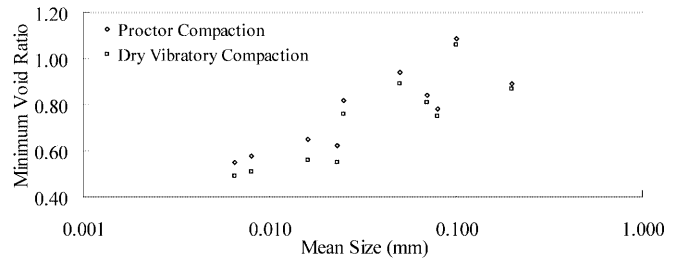


Fig. 7. Minimum void ratio plotted against mean size

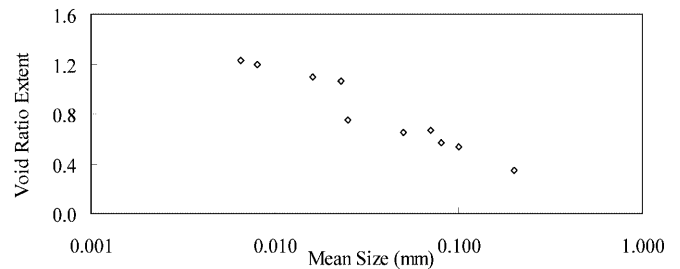


Fig. 8. Variation of void ratio extent with mean size

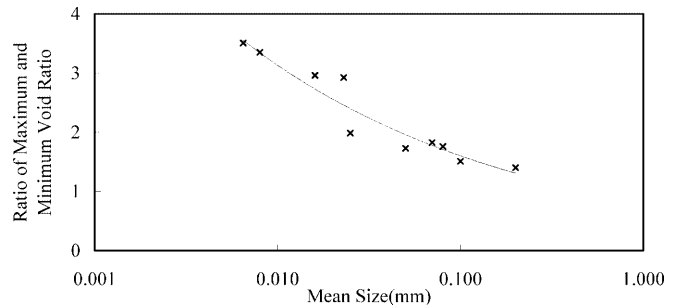


Fig. 9. Ratio of maximum and minimum void ratio plotted against mean size

Proctor compaction

Proctor compaction test was conducted on various ash samples to find out the relation between the compaction properties and the grain size distribution. With increasing fineness, the maximum dry density increases (Fig. 10) and the optimum moisture content decreases (Fig. 12). The decrease of the optimum moisture content with increasing fineness is contrary to the observed phenomenon for natural soils of similar grain size distribution. Coal ash has a variation of dry density with moisture content that is smaller than the variation of well-graded soils with the same median grain size [9]. Normal soils have air voids between 1 and 5% at maximum dry density, while ash contains 5–15% air voids at maximum dry density [17]. The minor variation of the dry density of ash with increasing moisture is explained by the air void content of ash as high as 20% in the present case.

In fine ashes (Fig. 1b), less gas is trapped in the fused state, so that the specific gravity will be higher and particles will be smoother, achieving a maximum dry density at a lower moisture content. High void contents of ash are generally associated with a higher coefficient of uniformity (Fig. 11) and the presence of porous particles in the coarse fraction. High void contents allow the coarse ash (Fig. 1a) to be compacted over a higher moisture content (Fig. 12).

Coal ash does not experience a density increase of same magnitude as are experienced by fine-grained soils from comparable changes in the compactive effort. Bottom ash shows a significant density increase under a modified Proctor compaction. This is the result of partial crushing of the porous bottom ash particles under heavy energy input ([5], [6], and [7]).

Permeability

The permeability of coal ash was determined at the Proctor density by the falling head method, in which water is allowed in the sample through a constant diameter vertical standpipe until the falling level in the vertical tube reaches a previously established mark when the timer is set in operation. The head continues to fall at a decreasing rate until a second mark is passed, when upon the timer and the flow both are stopped. The permeability of the ash is calculated from the known data of the cross sectional area of the vertical stand pipe and that of the sample, initial total head difference across the sample, and head difference at time recorded by the timer. The permeability-

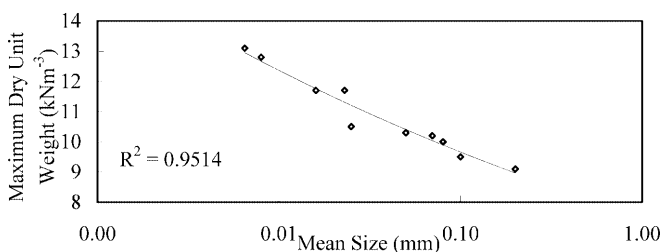


Fig. 10. Maximum dry unit weight (Proctor) plotted against mean size

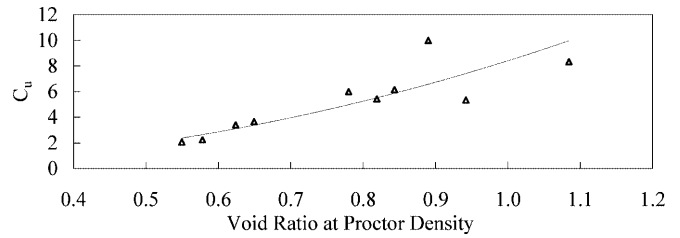


Fig. 11. C_u Plotted against minimum void ratio of proctor density

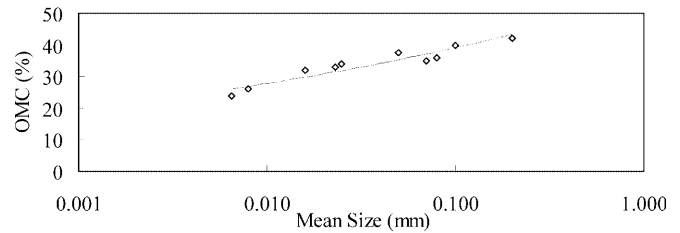


Fig. 12. Optimum moisture content (Proctor text) plotted against mean size

ty of the ash depends on its particle size distribution and its void ratio. Ash is loosely deposited in the pond. As a result, the values of permeability are higher in ash ponds due to a very high void ratio. The permeability of compacted ash is related to the effective size or the mean sizes at Proctor density (Fig. 13). The coefficient of reliability for the effective sizes was found to be 0.89 as compared to 0.85 for the mean size of the ashes. The permeability k is expressed as a function of grain sizes at Proctor density as:

$$k = 0.054 (D_{10})^{1.1} , \tag{2}$$

$$k = 0.0026 (D_{50})^{0.62} , \tag{3}$$

where the unit of k is mm s^{-1} , D_{10} is the effective size and D_{50} is the mean size in mm.

Attempts were made to relate the permeability of ash samples with the void ratio (Fig. 14). At the maximum void ratio, it may be several times that of the permeability at Proctor density. However in the loose state, internal erosion plays a greater role than the permeability.

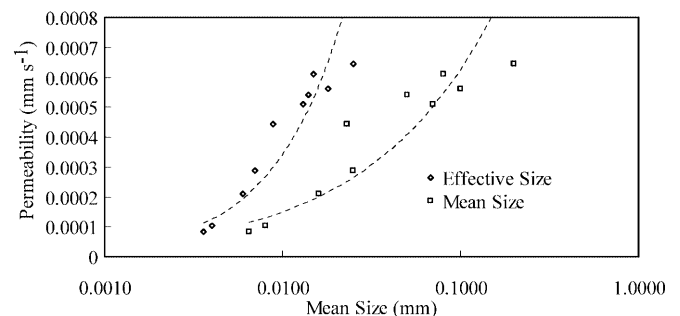


Fig. 13. Variation of permeability of ashes at proctor density with mean sizes

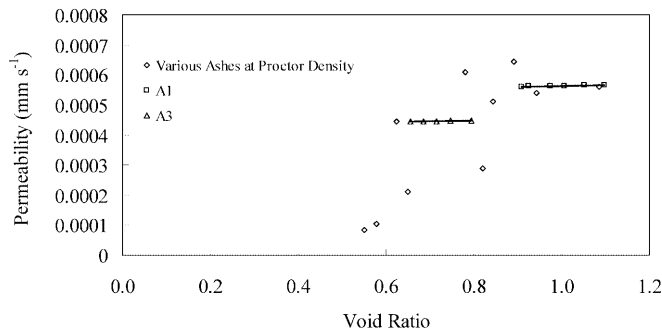


Fig. 14. Variation of permeability with void ratio

Compressibility

Compressibility is an important parameter to estimate the settlement of a ground in stressed conditions. The compressibility of ash was estimated in a 60-mm diameter and 20-mm thick oedometer ring on the reconstituted loose dry samples. Samples were prepared in the oedometer ring by the dry pluviation method. The dry ash was funneled with a zero potential energy in the ring to obtain samples with the loosest possible density. The sample was then pressed under a surcharge of 1 kPa and filled-in to obtain a desired specific volume. The specific volume is defined as the volume of ash sample containing unit volume of the ash grains. All reconstituted ash samples show a common pre-consolidation pressure of 100 kPa probably because of the exposure of the ash material to a common thermal stress in the combustion furnace during formation. With increasing coarseness the compression of coal ash closely resembles that of sandy soils. There is certain evidence of grain crushing with increasing effort in tests on coarse ashes [18].

At higher consolidation pressures the compression curves of fine ashes (B5, B6, and B7) may be represented by a unique normal consolidation line (ncl) and their specific volume may be determined by the current state of stress (Fig. 15). There is a progressive increase in the stiffness with decreasing initial specific volume. The stiffness is higher for the samples having a void ratio close to their minimum void ratio.

The slope of the loading line (V_s -log p plot) in 1-to 100-kPa range depends upon the placement

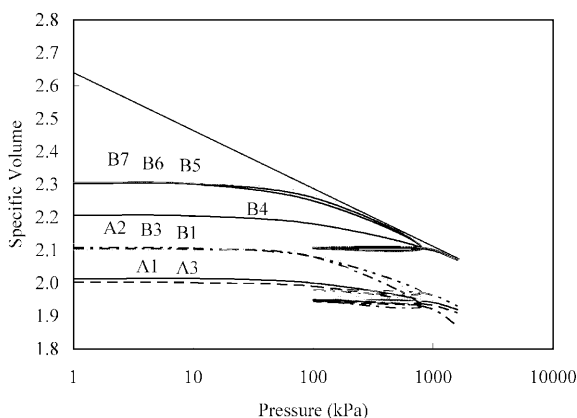


Fig. 15. Specific volume plotted against the pressure for various ashes

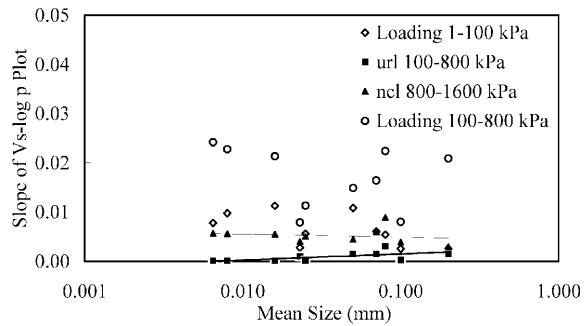


Fig. 16. Variation of slope of ncl and url with mean size

specific volume of the ash. For the loading curve in the range of 100–800 kPa, the slope tends to stabilize. The trend slope of the normal consolidation line (ncl) in the range of 800–1600-kPa decreases with increasing mean sizes (Fig. 16). The trend slope of the unloading reloading line (url) at 100-to 800-kPa increased with increasing mean sizes neglecting hysteresis. The ratio of the slopes of ncl and url does not indicate any definite trend, however, considerable advantage in understanding can be gained by analyzing the effect of fines or the occurrence of crushing. Ashes that are predominantly fine show a minimum void ratio significantly lower than coarse ashes. Compression beyond 800 kPa tends to pack them to a denser state than that obtained by vibration and there is negligible rebound on unloading (Fig. 17).

Some anomalies overtly exist in the behavior of A3 and B4 ash samples having similar mean sizes. The presence of a significant percentage of coarse particles in the finer matrix leads to a rebound on unloading. The presence of porous particles, as expected in the floating scum, may reduce the rebound to insignificant levels due to crushing. The coal ashes having a compression index C_c , in the range of 0.006 to 0.01 and recompression index C_{cr} , between 0.0003 and 0.003, show significant stiffness to dry compression in the oedometer that further increases in the un-loading re-loading cycle. It implies that virgin compression may lead to significant gains in the stability of an ash dump.

Angle of repose

There exists a close relation between the angle of repose (ϕ_r) and the grain characteristics of granular soils.

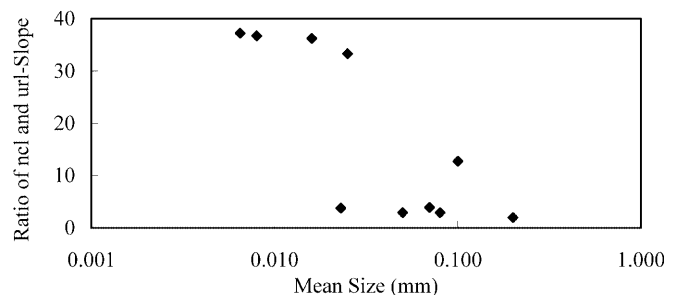


Fig. 17. Ratio of ncl and url-slope plotted against mean size

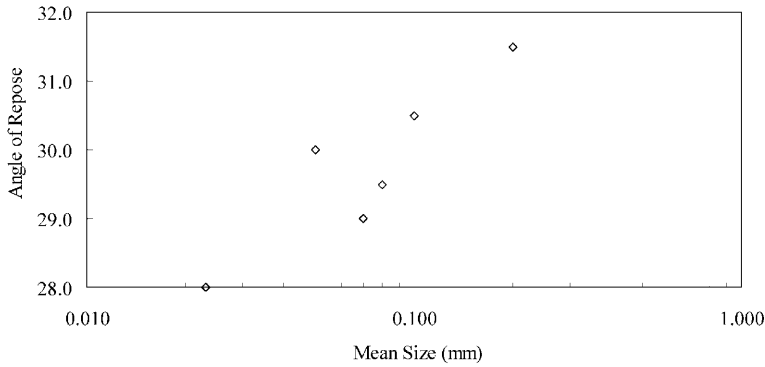


Fig. 18. Angle of repose plotted against mean size

Terzaghi [19] and Taylor [20] interpreted the angle of repose as a kind of angle of internal friction obtained in the limiting conditions. Miura et. al. [2] suggested that the angle of repose of sands corresponds to the angle of internal friction in the loosest state at a limiting confining pressure. A procedure is standardized for the measurement of the angle of repose of ashes.

The angle of repose was measured on a flat surface by slow pouring through a funnel and a sieve, keeping a distance of 20 mm between the deposit level and the pouring end. The average angle of repose of at least three tests on each ash was plotted with the mean size (Fig. 18). The angle of repose for the ashes under consideration varies in the range of four degrees. The angle of repose of coal ash increases with the mean size (Fig. 18). There is a little or no effect of the coefficient of uniformity on the angle of repose of the sands [2]. It may be noted that fine ashes show a poor reproducibility in the angle of repose due to the formation of agglomerates.

Peak friction angle

The peak friction angle was estimated for the selected ashes with varying relative densities in a dry state with the direct shear test. The shear strength of coal ash is initially a nonlinear function of the overburden pressure with zero cohesion intercept. The peak friction angle results are plotted (a mean of five tests at each relative density) demonstrating a linear variation at a normal stress of 100 kPa. Coarse ash A1 shows a slightly lower friction angle as compared to the finer ash A2; see the best fit drawn in Fig. 19. A close observation of the best-fit equation reveals fitting constants having friction intercepts of 27.6 and 28.1 for A1 and A2, respectively at zero relative density. Its physical meaning is associated with the angle of repose. No definite trends are observed for the frictional properties of ashes in relation to their mean grain sizes. A general explanation is offered in terms of the stress-dilatancy and the packing state dependence of the peak angle of friction. Normally a loose ash contracts and a dense ash expands as it approaches the critical state, generally defined as shearing without change in shear strength or in volume. The critical state was found to be independent of the initial density and the confining pressure. The triaxial shear test results [11] of various ashes indicated a peak angle of internal friction corresponding to a relative density

(RD) and a mean confining pressure (p) for these tests. The critical angle was obtained by shearing ash samples to the axial strains in excess of 30%. The values of the fitting parameters (Q and r) were obtained from several triaxial shear tests (Fig. 20). The value of Q for coal ash is found to be 7.7. The value of Q and r for clean quartz sand is reported as 10 and 1 respectively [4]. The critical angle for coal ash, a morphological mineralogical parameter, was observed in a range of 22° for fine ashes and 30° for coarse ashes. As per Bolton [4], in the triaxial test conditions a relation among the peak and the critical angles of friction exists. It is conveniently expressed as,

$$Q \cdot RD - r = 0.33(\phi_p - \phi_c) + RD \cdot \ln(p) \quad (4)$$

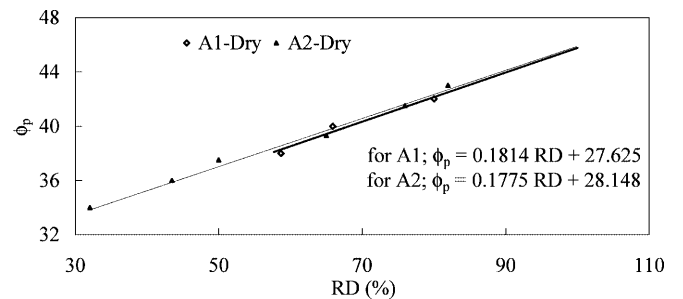


Fig. 19. Peak friction angle plotted against relative density

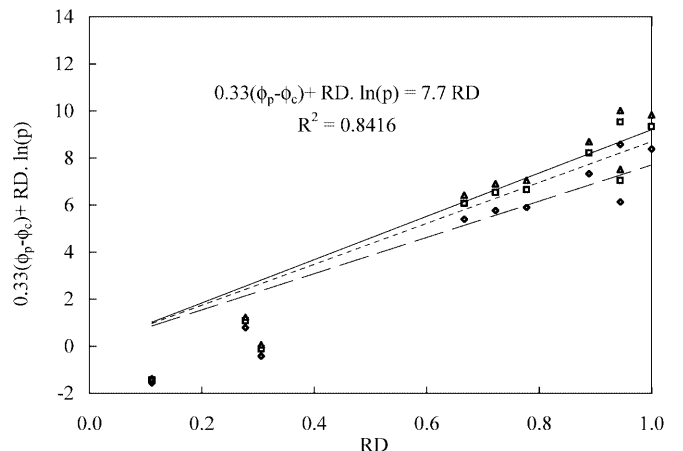


Fig. 20. Variation of fitting constants for ash

Table 1. Grade of correlation between grain size and properties of coal ash

Grade of correlation	C_u	G_a	e_{\min}	e_{\max}	e_{\min}/e_{\max}	$\gamma_{\max \text{ Proctor}}$	OMC	k	k	ncl-slope	url-slope	ϕ_r	ϕ_p	Q
	D_{50}	D_{50}	D_{50}	D_{50}	D_{50}	D_{50}	D_{50}	D_{50}	D_{10}	D_{50}	D_{50}	D_{50}	D_{50}	D_{50}
R	♣	∧	∧	∨	♣	♣	♣	∨	∧	∨	∧	∨	∨	~

where ϕ_p and ϕ_c are the peak and critical angles of friction, Q and r are material fitting parameters uniquely represented for an ash, RD is the relative density and p is the mean confining pressure in the units of kPa. The estimates of Q on the basis of equation (4) and experimental observations of ϕ_p , ϕ_c , RD and p are presented in Fig. 20 selecting r as zero. The coefficient of reliability presented in Fig. 20 improves further on rejection of low density data points.

Conclusions

The characteristics and properties of coal ashes were investigated in the present work. This knowledge is useful for the engineering community involved in geotechnical applications of coal ash. This paper highlights the need for a mechanical model or a tool for analysis that attempts to capture primary, secondary and index properties of ash material from physical and chemical properties. The critical state, that is recognized to be independent of environmental conditions, is an intrinsic parameter related to constitution and general nature of the particle surface. The mean grain size was studied in relation to the various properties of the ash material to find the grades of correlation, R (interpreted from the coefficient of reliability, R^2 ; Table 1) such as outstanding (♣), reasonable (∧), poor (∨), and independent (~).

Based on the test results, various characteristics of ash are briefly summarized:

1. The ashes sampled for the study have a common mineralogical origin. The uniformity coefficient is larger for the ash collected near the location of its discharge, when compared to the ash collected far away; where the ash is generally fine. The fine ashes have slightly higher apparent specific gravity than the coarse ashes. The void ratio extent, i.e. a difference of e_{\max} and e_{\min} , or a ratio of e_{\max} and e_{\min} , decreases with an increase of the mean size.
2. The maximum densities obtained in dry vibration and Proctor tests differ for fine ashes. The maximum dry density decreases and the optimum moisture content increases with the mean size increasing.
3. The permeability of ash at the Proctor density is more appropriately related to the effective size than to the mean size. There is a scatter in the relation of permeability and void ratio because of the presence of pores in the ash particles.
4. The ashes indicate a pre-consolidation pressure of 100 kPa. The slope of V_s -log p plots of normally consolidated ashes beyond a loading of 800 kPa shows a decreasing trend with increasing mean size. The unloading-reloading plot suggests induced stability of

ashes due to pressing. The slope of the unloading-reloading plot indicates elastic rebound, which generally increases with increasing mean size.

5. The angle of repose increases with the mean size for coarse ashes.
6. The peak friction angle is a function of the relative density, the mean confining pressure and the material characteristics controlling the critical angle.
7. The coal ashes show a lower value (7.7 & 0) of material fitting parameter Q and r as of clean quartz sands (10 & 1).

List of notations

ϕ_c, ϕ_r, ϕ_p	critical angle, angle of repose and peak angle of friction for ash.
$\gamma_{d \max}$	maximum dry unit weight in dry vibration test.
$\gamma_{d \max \text{ Proctor}}$	maximum dry unit weight in Proctor test.
γ_{\min}	minimum dry unit weight.
θ	diffraction angle in degree.
C_c, C_r, C_s	compression, recompression, and swelling index in dry state.
C_u	uniformity coefficient.
D_{10}	size of which 10% particles are finer.
D_{50}	mean size.
ESP	electrostatic precipitator.
e_{\max}, e_{\min}	void ratio corresponding to loosest state and densest state.
A1, A2	ash obtained from ash pond location -1, 2 respectively.
A3	composite ash obtained from out let of ESP
AU	intensity of x-ray diffraction in arbitrary units
B1 to B7	ash obtained in dry state from ESP hopper location 1 to 7.
G_s, G_a	specific gravity of solids, apparent specific gravity.
k	permeability.
ncl	normal consolidation line in V_s -log p plot.
OMC	optimum moisture content.
Q, r	fitting parameters.
p	overburden pressure in oedometer test & mean confining pressure in triaxial test (kPa).
R, R^2	grade of correlation, coefficient of reliability.
RD	relative density.
url	unloading reloading line in V_s -log p plot.
V_s	specific volume.

References

1. R. Spronck, Proc. 2nd ICSMFE, 3 (1948), p. 15
2. K. Miura, K. Maeda, M. Furukawa, & S. Toki, Soils and Foundations, 37(3) (1997), p. 53
3. T. Iwasaki & F. Tatsuoka, Soils and Foundations, 17(3) (1977), p. 19
4. M. D. Bolton, Geotechnique, London, 36(1) (1986), p. 65
5. G. A. Leonards & B. Bailey, JGE, ASCE, 108(GT4) (1982), p. 517
6. P. S. Toth, H. T. Chan, & C. B. Crag, Can. GTJ, 25 (1988), p. 594
7. K. M. Skarzynska, A. K. M. Rainbow, & E. Zawisza, Proc. 12th ICSMFE, 3(1) (1989), p. 1915
8. U. Dayal, Ash Pond & Ash Disposal system, (Ed.) Narosa, New Delhi, (1996), p. 143
9. A. Sridharan, N. S. Pandian, & S. Srinivas, Ash Ponds and Ash Disposal System, (Ed.), Narosa, New Delhi, (1996), p. 97
10. A. Trivedi, Ph.D. Thesis, Thapar Institute of Engineering and Technology, Patiala, India (1999)
11. A. Trivedi, V. K. Sood, P. K. Bajpai, & J. Singh, Report, PSCST, Chandigarh, India (1996)
12. S. Raymond & P. H. Smith, Civil Eng. and Public Works Rev, Morgan-Grampian, London (1966), p. 1107
13. S. Raymond, Proc. Inst. Civil Engineering, 19 (1961), p. 515
14. S. Torrey, Noyes Data Corporation (Ed.), Park Ridge, NJ, USA (1978)
15. R. K. Seals, L. K. Moulton, & B. E. Ruth, JSMFD, ASCE, 98(SM4) (1972), p. 311
16. N. S. Pandian, C. Rajasekhar, & A. Sridharan, JTEVA, ASTM, 26(3) (1998), p. 177
17. K. L. Moulton, West Virginia University, Morgantown, WV, USA (1978)
18. D. L. Webb, Proc., 8th ICSMFE, Vol. 1.2, Moscow, (1973), p. 471
19. K. Terzaghi, Wiley, New York (1943)
20. D. W. Taylor, John Wiley, New York (1948)